



AstroGeoVis v1.0: Astronomical Visualizations and Scientific Computing for Earth Science Education

Tihomir S. Kostadinov¹

¹Department of Liberal Studies, California State University San Marcos, 333 S. Twin Oaks Valley Rd., San Marcos, CA 92096, USA

Correspondence: Tihomir S. Kostadinov (tkostadinov@csusm.edu)

Abstract. Modern climate science, Earth system science, physical geography, oceanography, meteorology, and related disciplines have increasingly turned into highly quantitative, computational fields, dealing with processing, analysis and visualization of large numerical data sets. Students of these and many other disciplines thus need to acquire robust scientific computing and data analysis skills, which have universal applicability. In addition, the increasing economic importance and environmental significance of solar power and sustainable practices such as passive building design have recently increased the importance of understanding of the apparent motions of the Sun on the celestial sphere, for a wider array of students and professionals. In this paper, I introduce and describe *AstroGeoVis v1.0*: open-source software that calculates solar coordinates and related parameters and produces astronomical visualizations relevant to the Earth and climate sciences. The software is written in MATLAB®; while its primary intended purpose is pedagogical, research use is envisioned as well. Both the visualizations and the code are intended to be used in the classroom in a variety of courses, at a variety of levels (targeting high school students to undergraduates), including Earth and climate sciences, geography, physics, astronomy, mathematics, statistics and computer science. I provide examples of classroom use and assignment ideas, as well as examples of ways I have used these resources in my college-level teaching.

Dedication

Tihomir S. Kostadinov dedicates this paper to the memory of his parents, who instilled in him a deep interest in and appreciation of astronomy, mathematics, and science.

1 Introduction

The total radiant energy coming to Earth from our star, the Sun, and its spatio-temporal patterns, are the first order factors determining planetary habitability, climate and seasonality on Earth's surface. Energy from the Sun powers processes such as weather and ocean currents, as well as virtually the entire modern biosphere via oxygenic photosynthesis. It is therefore important for students of Earth sciences to develop a rigorous and quantitative understanding of the factors that influence incoming solar radiation, or insolation, variability over various spatio-temporal scales, from the local and seasonal, to the global and long-term, e.g. involving the Milankovitch cycles (e.g. Berger et al. (2010) and Kostadinov and Gilb (2014)). In



addition, the increasing importance of renewable energy sources such as solar photovoltaics and innovative energy-efficient passive building design requires that an increasing variety of professionals be familiar with concepts such as solar declination and the daily and annual path of the Sun on the celestial sphere.

Earth sciences, similarly to many disciplines, have become increasingly quantitative in nature over the last few decades; there has been a significant increase in the generation and subsequent analysis of large quantities of data coming from a variety of sources, from *in-situ* electronic instruments to satellite remote sensing and climate models. The processing and analysis of these numerical data sets requires various levels of Information Technology (IT) and computational skills. It is thus becoming increasingly imperative to teach basic computational skills to a wide variety of majors, including those not necessarily in Science, Technology, Engineering and Mathematics (STEM) disciplines. For those in STEM fields, it is even more imperative that scientific computing be an integral part of the curriculum. It is best if such skills are taught organically in conjunction with the introduction of various concepts from the discipline itself. For example, instead of just teaching the path of the Sun in the sky and its seasonal variation with a static figure, educators should strive to introduce the algorithm (and often - the data) behind the concept. This empowers students to gain deeper understanding of the controlling variables, and to learn how to do the computations, manipulations of equations and data, and visualizations themselves. Of course the level and depth at which these concepts are taught will depend on the grade level and prior preparation of the student body. This approach also empowers instructors, who themselves gain a deeper understanding of the subject matter, and have the flexibility to create dynamic figures and animations on demand for their classes.

Here, I describe *AstroGeoVis v1.0*, scientific software that performs astronomical computations and produces visualizations of relevance for the geosciences and solar energy applications. The code was written in the MATLAB® scientific computing language for pedagogical purposes and arose naturally as the author was seeking to improve his own positional astronomy knowledge base, and to produce visualizations and assignments for his Introduction to Physical Geography and Introduction to Oceanography classes. The author has a longstanding interest in pedagogical applications of scientific visualizations, exemplified by the earlier development of the Earth Orbit Model (Kostadinov and Gilb (2014)). Many geophysical and astronomical concepts require good quantitative, IT and 3D spatial thinking skills to master. A significant advantage of *AstroGeoVis v1.0* that greatly increases its pedagogical utility is that it addresses all these aspects of learning since it comes with open-source code where computational algorithms can be inspected, and many of the visualizations are 3D objects in their native MATLAB® environment, and thus have pan-tilt-zoom (PTZ) capability. Furthermore, *AstroGeoVis v1.0* is dynamic, and can be modified and adapted as needed by instructors and/or students. For example, instructors can generate figures on demand for different latitudes and solar declinations, and math and computer science students can be tasked with studying and modifying the algorithms. Ideas for assignments are discussed below and in the code.

In the following sections, I describe the components of *AstroGeoVis v1.0*, with an emphasis on pedagogical utility. The basic logic and algorithms used are described briefly, with more details in the commented code. The underlying astronomical algorithms used are those of *Astronomical Algorithms* by J. Meeus (Meeus (1998)). The code presented here was developed by the author based on first principles and the aforementioned astronomical algorithms in Meeus (1998), and some other references as cited herein or in the code. Many tools providing similar astronomical information exist, and some such tools/sources



are listed in Sect. B. They can be used to study alternative approaches and further verify *AstroGeoVis v1.0*. The code has been extensively tested. The author welcomes suggestions for additions and improvements, and notifications of any possible remaining errors, at the contact information provided.

2 Description of *AstroGeoVis v1.0* Components with Illustrative Examples & Pedagogical Applications

2.1 Solar Declination Student Project

In this section, I present a semester-long student project in which students are asked to measure the altitude and azimuth of the Sun on a weekly basis. The measurements are performed using widely available materials, namely any straight stick-like object (I use a 60 cm PVC pipe) that can serve as a gnomon to cast a shadow, a measurement tape, and a protractor. Students measure the shadow length and the azimuth of the shadow direction. At the end of the semester, students analyze their data and use their measurements to determine the declination of the Sun and track and discuss its progress throughout the semester. Two variants of the project are presented. In the first variant, students make the measurements at any time of day and record both the altitude and the azimuth of the Sun. An additional requirement for this variant is that the direction of true North needs to be predetermined and known to the students before the start of the measurements. In the second variant, students make the measurements at local solar noon and record only the shadow length. They are tasked to determine local solar noon for the dates and location(s) of their measurements. This variant greatly simplifies the relationship between declination and solar altitude and the interpretation of students' results.

The end of semester analysis for the first variant is accomplished in the MATLAB® script template `solar_declination_Exercise.m`. Students import their data from a text file and either use the provided formulae to compute solar altitude and declination from their measurements, or they can be tasked with deriving or looking up the formulae. The altitude of the Sun, h , is determined as:

$$h = \tan^{-1} \left(\frac{g}{s} \right) \quad (1)$$

where g is the gnomon length, and s is the shadow length from the base of the gnomon to the tip of the shadow, expressed in the same units as g . The gnomon has to be placed vertically on a horizontal level surface. Subsequently solar declination, δ , is determined using conversion from local horizontal to equatorial coordinates (Vincent (2003)):

$$\delta = \sin^{-1}(\sin h \sin \phi + \cos h \cos \phi \cos A) \quad (2)$$

where h is solar altitude, ϕ is the latitude of the observer, and A is the measured azimuth of the Sun. Note that here and throughout *AstroGeoVis v1.0* I define azimuth as measured clockwise from true North, unlike Meeus (1998) (see his Ch. 13), and as in Vincent (2003).

The analysis for the second variant is achieved using an Excel® spreadsheet, a template for which is provided with *AstroGeoVis v1.0*. The second variant is more suitable for non-STEM students who may not have the required aptitude and background to deal with scientific code or more advanced trigonometry/geometry. Both variants are provided with comments

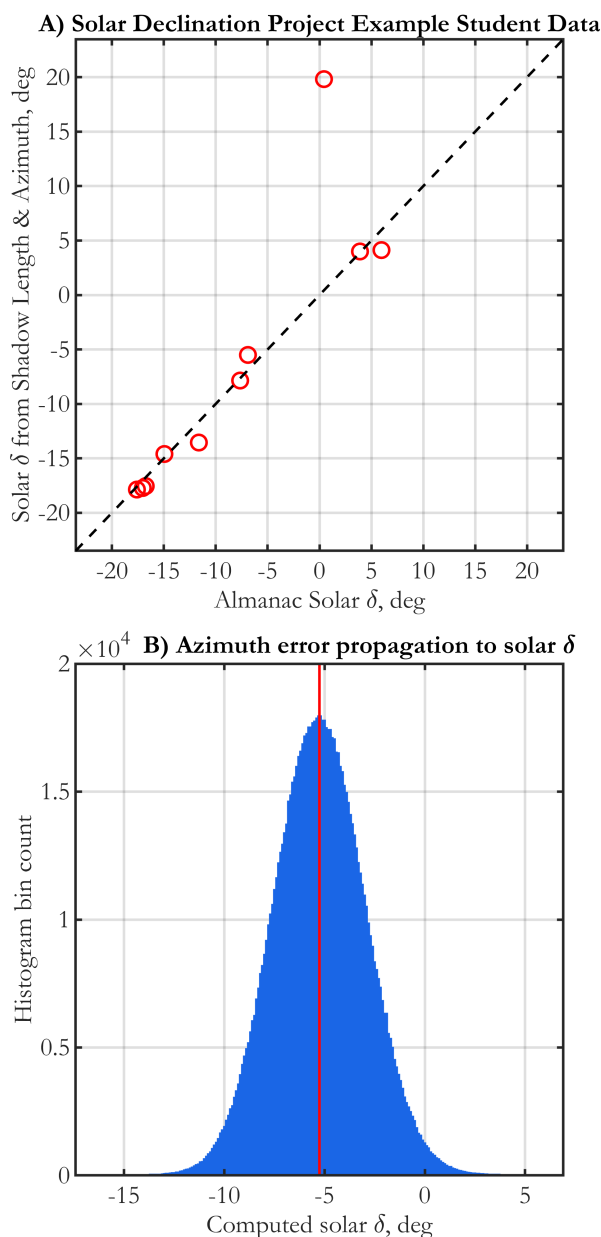


Figure 1. (A) Examples of solar declination (δ) data computed from student-gathered observations of altitude, h , and azimuth, A , of the Sun (y-axis), as compared to almanac values (USNO (2020)) (x-axis). (B) Results of one million Monte Carlo simulation runs used to propagate uncertainty in measured azimuth to the computed declination. The histogram of resulting δ values is shown, $\delta = -5.26^\circ$ is indicated as a vertical red line; this is the value computed from the assumed mean $A = 250^\circ$, using a fixed shadow length of 175 cm cast by a gnomon of length 61 cm. The input azimuth is assumed to have a standard deviation of 3° . Plots are produced by the scripts `solar_declination_Exercise.m` for panel A and `solar_declination_Monte_Carlo.m` for panel B.



90 and ideas for additional questions and tasks for the students. In my teaching experience, I have used both variants multiple
 times with success. Students are best split into groups of two. Most student measurements result in excellent determinations
 of solar declination as compared to almanac values (Fig. 1A). Students can also be asked to discuss sources of measurement
 error and do uncertainty propagation. Monte Carlo simulations are used to propagate random measurement error to solar dec-
 lination, as illustrated by the `solar_declination_Monte_Carlo.m` script; an example result is shown in 1B. This task
 95 is suitable for more advanced students, or students in computer science, mathematics or statistics. Students can also be asked
 to vary both inputs simultaneously in the Monte Carlo simulation, and/or to do analytical error propagation (e.g. see Supple-
 ment to Kostadinov et al. (2016)). Multiple aspects of this project are useful and foundational pedagogically, such as hands-on
 field/measurement experience, determining one's geographic coordinates and looking up relevant technical information, per-
 forming subsequent data analysis and interpretation of results (including comparison with theoretical expectations and almanac
 100 (i.e. modeled) values), plotting, and error analysis.

2.2 Daily Path of the Sun on the Celestial Sphere

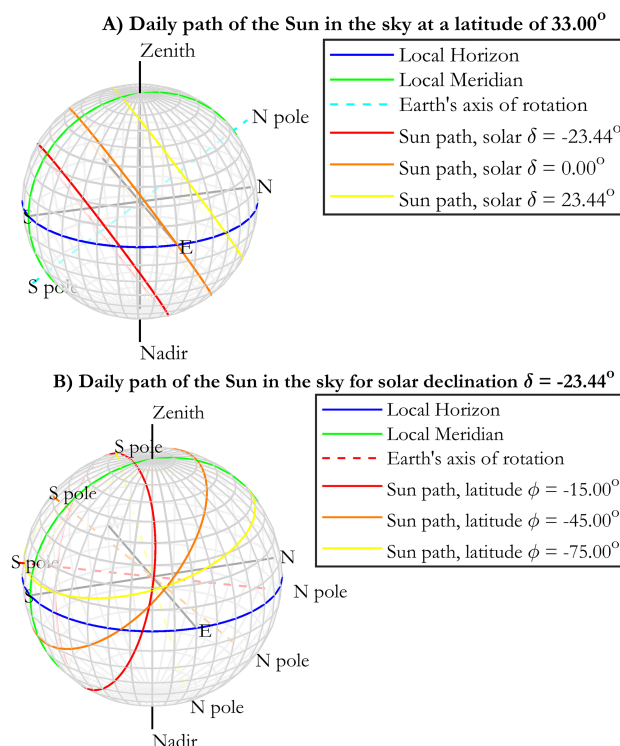


Figure 2. Example 3D plots of the daily path of the Sun on the celestial sphere; multiple solar declination cases are plotted in (A), whereas multiple latitude cases are plotted in (B). Plots are produced by the function `sun_path.m`.



The daily path of the Sun on the celestial sphere at a given location and its annual variation have important implications for local insolation and climate, duration of daylight, and thus also for agriculture, solar renewable energy, passive building design and related applications. It is a function of the latitude of the observer and the declination of the Sun, and figures depicting its seasonal variation are common in introductory physical geography textbooks, e.g. *Geosystems* (Christopherson (2011)).

Here, I present the `sun_path.m` function, which plots one or more apparent daily Sun paths by first generating a time series of solar horizontal coordinates for a 24-hr period and then converting them to Cartesian coordinates for plotting. One way to call the function is to input a single latitude and one or more declination values (an example is given in Fig. 2A). The observer is located at the center of the grey semi-transparent mesh sphere, which represents the celestial sphere with the local horizontal coordinate system grid. The local horizon and meridian are drawn, the zenith and nadir points are shown, as is Earth's axis of rotation, indicating the directions of the North and the South Pole. Users can also choose to specify a given scalar solar declination and plot the path of the Sun for several latitudes instead - an example is shown in Fig. 2B. These 3D figures with PTZ capability are valuable to improve students' spatial understanding of the phenomena; inputs can be varied in real time.

2.3 The Terminator

The terminator is the curve on Earth's along which sunrise or sunset is occurring at a given moment. Here I present a collection of functions visualizing the terminator and creating animations of its progression on Earth's surface over a single day, or over an entire year. An example of a static plot of the terminator is shown in Fig.3. In addition to the line of the terminator, the locations of the sub-solar and anti-solar points are shown, and the meridian at which the Sun is transiting is drawn, as is the opposite meridian 180° away. In addition, the altitude of the Sun is also mapped.

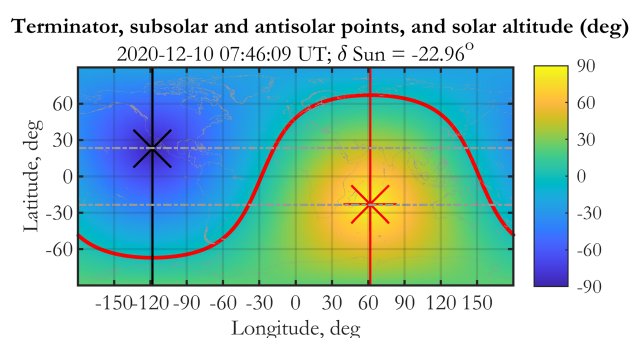


Figure 3. An example plot of the terminator, produced by the `terminator_shaded_altitude.m` function. The terminator is drawn as a red line, the subsolar point is a red 'x', and the anti-solar point - a black 'x'. The meridian of local solar noon (red) and its opposite meridian (black) are also drawn.

The global map of the terminator (Fig. 3) has a multi-faceted pedagogical value, and I have used it in my classes to illustrate concepts such as sunrise and sunset, day length, altitude of the Sun, rotation of Earth, time and time zones, the seasons and their effect on the location of the sub-solar point. The animations add significant pedagogical value to the static



plot of Fig.3. The function `terminator_video_daily_shaded_altitude.m` produces an animation of the terminator over a given 24-hour period and is useful for illustrating the day-night cycle on Earth and time zones. The function `terminator_video_annual_shaded_altitude.m` produces an animation of the terminator over an entire year and is valuable in illustrating seasons and their phase shift between the Southern and Northern Hemispheres, day length, and the sub-solar point. The animation also illustrates the analemma (Sect. 2.4). Example videos are included with *AstroGeoVis v1.0*.

The method chosen for producing the terminator map is itself useful pedagogically (as are virtually all parts of *AstroGeoVis v1.0*), especially for astronomy, math and computer science students, as well as for teaching scientific computing skills in the geosciences. Briefly, the declination and right ascension of the Sun are determined for the chosen moment using the Meeus (1998) algorithms. The terminator is then parameterized as the equatorial great circle in a geocentric Cartesian coordinate system, in which the sub-solar and anti-solar points are the poles. Solar declination and the longitude of the meridian where the Sun is transiting are then used to generate the appropriate 3-D rotation matrix to transform the terminator coordinates to the geographic latitude/longitude system.

Solar altitude is then computed on a latitude/longitude grid by first determining the local sidereal time, s (Meeus (1998)), and using it to compute the local hour angle of the Sun, HA (Meeus (1998)):

$$HA = s - \alpha \quad (3)$$

where α is the right ascension of the Sun. The variables in Eq. 3 must all be consistently expressed in either hours or degrees. The altitude of the Sun, h , is then determined at every grid point using the conversion from equatorial to local horizontal coordinates Meeus (1998):

$$h = \sin^{-1}(\sin \phi \sin \delta + \cos \phi \cos \delta \cos HA) \quad (4)$$

where ϕ is the latitude, δ is the declination of the Sun, and HA is the hour angle of the Sun.

Note that the location of the terminator determined by the functions presented here do not take into account atmospheric refraction and consider sunrise and sunset to be the moments when the center of the solar disk is at the mathematical horizon. The terminator plot and some other plots presented subsequently purposefully avoid the use of the term declination. In my experience, this makes them more suitable for use in classes such as Introduction to Physical Geography for non-STEM majors, where the use of technical astronomy terms may be undesirable. Conversely, declination and the fact that it is a governing variable for many of the visualizations and phenomena discussed here should be discussed in astronomy and physics classes, and in more advanced Earth science classes and those focusing on the computational methods.

2.4 The Equation of Time and the Analemma

Humans are influenced by a strong circadian rhythm and have used the motions of the Sun on the celestial sphere for timekeeping since ancient times. However, the Sun exhibits irregularities that cause, for example, time-varying corrections to be needed for sundials. These irregularities are captured by the concept of the Equation of Time, E , which is defined as the difference between the hour angle of the true Sun, HA_{true} and the hour angle of the mean Sun, HA_{mean} , (a fictitious Sun that moves at



a uniform rate along the celestial equator) (Meeus (1998)):

$$E = HA_{true} - HA_{mean} \quad (5)$$

The temporal variability in E is caused by 1) the eccentricity of Earth's orbit, and 2) the obliquity of the ecliptic, resulting in the true Sun not moving uniformly along the celestial Equator, i.e. the right ascension of the true Sun doesn't change at a uniform rate, and there are times of the year when the true Sun is ahead of the mean Sun, and vice-versa.

The script `analemma.m` computes and plots E and some related quantities using the right ascension and declination of the Sun as well as local sidereal time as given by the Meeus (1998) algorithms, sampled at a high temporal resolution. E is computed via Eq. 5 and Eq. 3. Further details of the computation can be found in the commented script. The resulting Equation of Time is given in Fig. 4A for 2021 (it looks practically identical for all years close to the present). E gives the correction needed for sundials. It reaches a maximum in early November, indicating that the true Sun is ahead of the mean Sun at that time of the year, explaining why the earliest sunsets of the year tend to occur before the December solstice in the Northern Hemisphere. When E is plotted against solar declination for an entire year, the analemma curve results (Fig. 5). It has the shape of a figure '8' and is often plotted on globes and in textbooks; it is also often demonstrated as a series of photographs of the Sun taken at the same civilian time at a given location throughout the year.

The time derivatives of the right ascension of the true Sun, α , and the Equation of Time, E , have instructional value. These two quantities are related as follows:

$$\frac{dE}{dt} = (k - 1) - \frac{d\alpha}{dt} \quad (6)$$

where $k = \frac{ds}{dt} = 1.00273790935 \text{ s/s}$ is the time rate of change of sidereal time, i.e. it's the ratio of the duration of the mean solar day to the duration of the sidereal day. Eq. 6 is derived by differentiating Eqs. 3 and 5 with respect to time and substituting one in the other, and noting that the time derivative of HA_{mean} is unity as long as the variables of Eq. 6 are all expressed in the same time unit.

The time series of the two derivatives in Eq. 6 (Fig. 4B, in minutes per day), illustrate that they are inversely proportional and offset by the values $k - 1$. The interpretation of these curves is as follows: the time derivative of E is zero when the solar right ascension is increasing at about 3 min 56 s per day (the amount of time by which the mean solar day is longer than the sidereal day), i.e. the true Sun is acting like the mean Sun. If the true Sun's $\frac{d\alpha}{dt}$ were always equal to $k - 1$, i.e. if the true Sun moved uniformly along the celestial Equator, then there would be no temporal variability in E . At times when $\frac{d\alpha}{dt} > k - 1$, the solar day is getting longer and the true Sun is lagging more and more behind the mean Sun, decreasing E (Eq. 5), and vice-versa.

The pedagogical value of the material and visualizations presented in this section is multi-faceted and is perhaps centered on illustrating the relationship between the orbital elements of Earth and Kepler's laws and their manifestation in the apparent motion of the Sun on the celestial sphere, resulting in practical applications, such as timekeeping. Details presented in this section generally go beyond what is suitable in an introductory undergraduate course in Earth Sciences and are more suitable for more advanced classes and students of astronomy, physics, mathematics, and computer science.

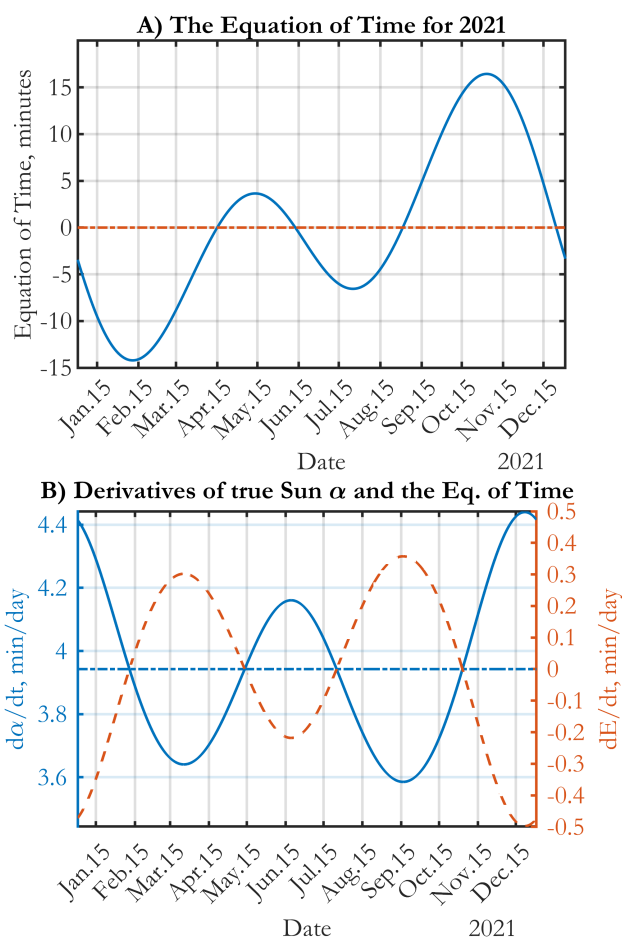


Figure 4. (A) The Equation of Time for 2021; (B) Time derivatives of the right ascension of the true Sun, α (left y-axis, blue solid curve), and the Equation of Time, E (right y-axis, red dashed line) for 2021. The value of $k - 1$ (Eq. 6) is plotted as a blue horizontal dash-dot line on the left y-axis. The function creating these figures is `analemma.m`

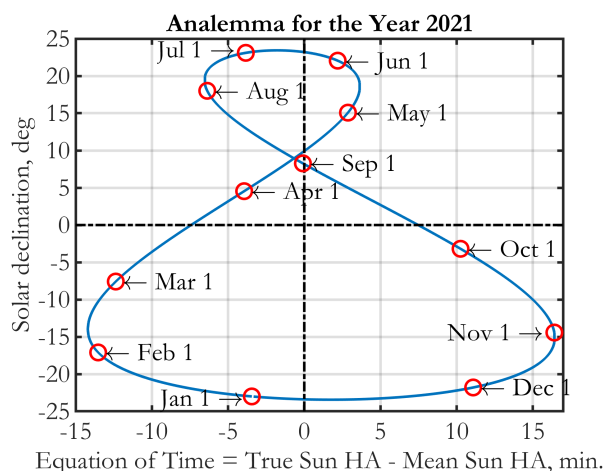


Figure 5. (A) The analemma for 2021, computed and plotted by `analemma.m`

2.5 Shadow of a Gnomon

Another interesting visualization that has pedagogical value is the gnomon shadow trace. More specifically, this is plot of the locus of points of the tips of the shadow cast by a vertical gnomon placed normal to a horizontal surface. The resulting curves are a function of latitude and the time of year (i.e. solar declination), and they can be explored over the course of a day, or over the course of a year at a given time of day. The former case is illustrated in Fig. 6A for a latitude of about 33°N at the time of the June solstice. This is a polar plot, in which the polar angle gives the azimuth of the direction of the gnomon shadow (referenced to true North), and the radial coordinate gives the shadow length for a 1 m long gnomon. The shadow tip points are color coded according to the time of day, making interpretation easier. Fig. 6B illustrates the gnomon shadow tip trace for a given location at the Equator for an entire year, color coded according to date. Because the moment chosen for the plot is at a fixed civilian time every day of the year, the resulting curve is in fact a projection of the analemma (Sect. 2.4); students can be asked to cross-check the analemma plot (Fig. 5) with these annual gnomon traces.

As with all *AstroGeoVis v1.0* code and visualizations, the gnomon plots and code are dynamic and adaptable and can be used in passive or active learning scenarios, e.g. instructors can just lecture using the figures, or they can ask students to come up with the algorithm, or to investigate the effects of latitude on the traces. Additionally, students can be tasked with designing a sundial using the principles in `gnomon_trace.m` as a starting point and taking into account the need for correction given by the analemma (Fig. 5 and Fig. 6B). Further details on sundial construction mathematics are given in Meeus (1998), Chapter 58.

2.6 Irradiance on a Tilted Solar Panel

Renewable solar energy and green/passive building design represent an increasingly important application area of concepts treated in *AstroGeoVis v1.0*. In this section I present functions that implementing a generic solution for the irradiance on a tilted

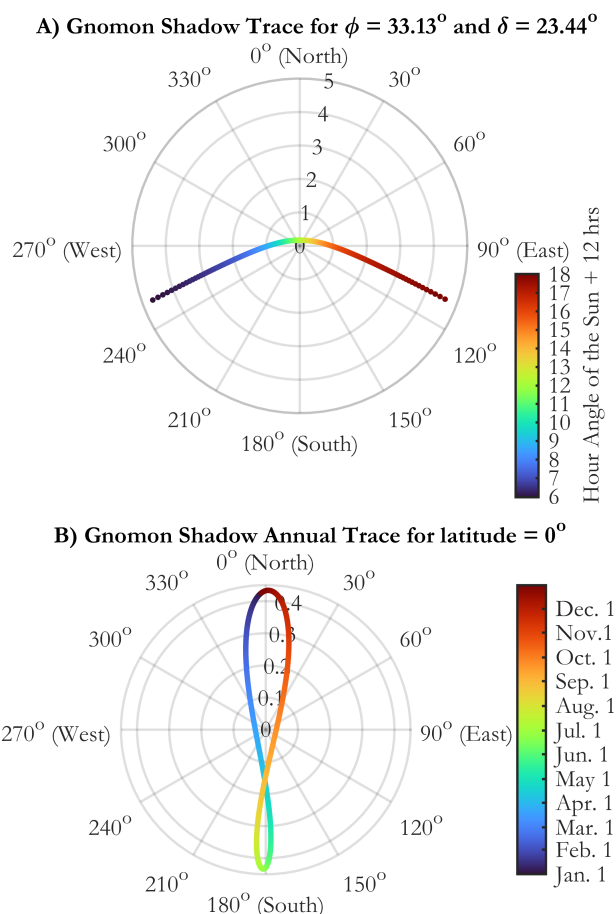


Figure 6. (A) Trace of the shadow tip of a vertical 1-meter gnomon on a horizontal surface at the default latitude of $\phi = 33^\circ 7' 45''\text{N}$, and for solar declination equal to the obliquity, i.e. the June solstice. The shadow tip points are color coded according to the time of day (color bar), given as the solar hour angle + 12 hours, i.e. 12:00 on the color scale corresponds to local solar noon. (B) Same as in A), but for all of 2021, at the times of local transit of the Mean Sun for every day, at the Equator and using the default meridian as specified in the function. Shadow tip points are color coded according to date. Panel A is produced by the function `gnomon_trace.m` and panel B - by the function `gnomon_trace_annual.m`



solar panel with any orientation, given its latitude and solar declination. Further, the functions compute total energy produced over the course of a year, and solve the optimization problem for maximizing energy production (Sect. 2.6.1). Irradiance is computed using first principles and the solar coordinates at high temporal resolution from the Meeus (1998) algorithms. Specifically, the direction toward the Sun, and the direction of the normal to the plane of the solar panel are expressed as 3D Cartesian vectors in the local horizontal coordinate system. Irradiance is computed by taking into account a) the Sun-Earth distance, r in relation to a distance of $r_o = 1$ AU, at which the total solar irradiance (TSI) $S_o = 1361 \text{ W m}^{-2}$ is defined (Kopp and Lean (2011); Prša et al. (2016)), and b) the angle, β , between the normal to the solar panel and the direction to the Sun, computed using the dot product of the vectors described above. Namely, the instantaneous irradiance, S , on the solar panel is computed as follows (e.g. see Kostadinov and Gilb (2014); Clack (2017)):

$$S(t) = S_o \left(\frac{r_o}{r(t)} \right)^2 \cos \beta(t) \quad (7)$$

where t is time, emphasizing that S , r , and β are functions of time. The angle β represents the solar zenith angle in a coordinate system for which the x-y plane is the solar panel plane. The short-term and long-term variability of S_o is not considered here, interested readers should consult, for example, Kopp and Lean (2011) and Foster et al. (2017) on this important topic.

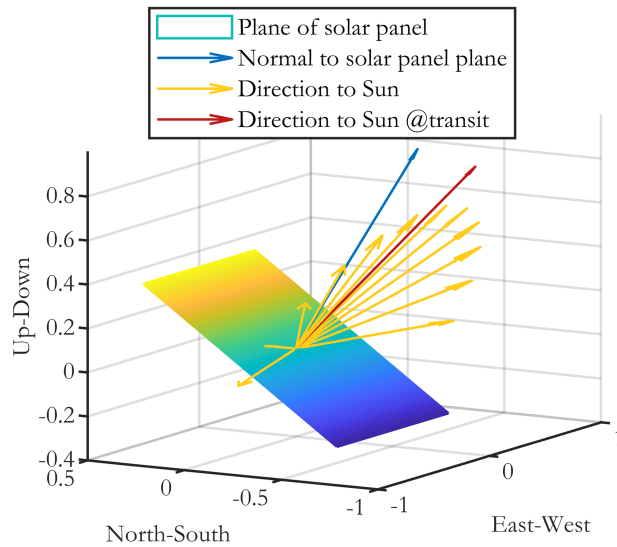


Figure 7. An example 3D plot of solar panel plane orientation with respect to the cardinal directions and the instantaneous direction towards the Sun. The normal vector to the solar panel plane is drawn in blue (longer vector). The direction towards the Sun is drawn in steps of one hour from approximately sunrise to sunset (yellow vectors), and the special case of local solar noon is separately drawn in red (longer vector). This figure is produced by the function `solar_panel_tilt_insolation.m`. The default values are used for this plot, as given in the function, namely solar panel facing true South and tilted ϕ degrees away from the vertical, where $\phi = 33^\circ 7' 45''$ N is the latitude. The date used is Oct. 25, 2020.

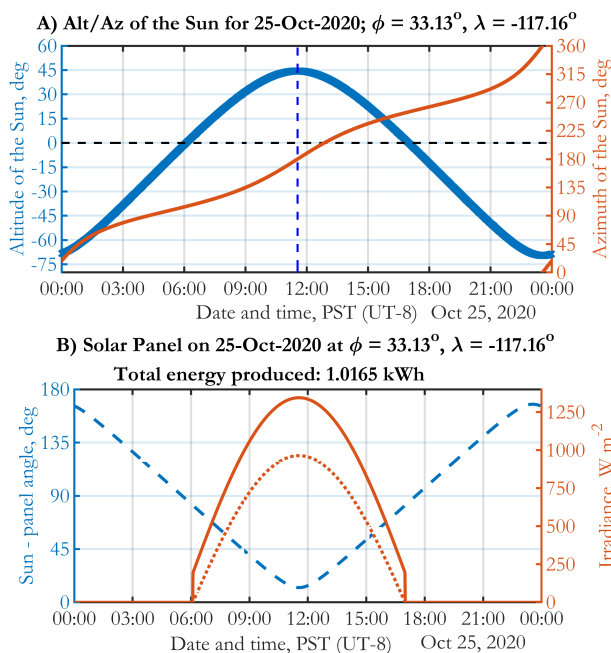


Figure 8. (A) Time series of the altitude (thick solid blue line on the left y-axis) and azimuth (thinner solid red line on the right y-axis) of the Sun for Oct. 25, 2020. (B) Time series of instantaneous irradiance on the solar panel surface (solid red line on right y-axis) and on a horizontal surface (dotted red line on right y-axis) for Oct. 25, 2020. The angle β (Eq. 7) is plotted as a dashed line on the left y-axis. The integrated daily total energy produced is shown in the panel title in kWh. The default values used for both figure panels are: the solar panel is facing true South and is tilted ϕ degrees away from the vertical, where $\phi = 33^\circ 7' 45''$ N is the latitude. Panel location is given in panel titles and used as defaults in the function producing both panels, namely `solar_panel_tilt_insolation.m`

Panel-Sun geometry and energy production over a given day is given by the function `solar_panel_tilt_insolation.m`, which computes Eq. 7 at chosen time steps and integrates it with respect to time over a day. Optionally, a 3D plot is produced showing the orientation of the panel, the normal to its plane, and the directions towards the Sun at local solar noon and in 1-hour steps from about sunrise to about sunset (Fig. 7). Also produced are time series plots of solar azimuth and altitude (Fig. 8A), and the angle β (Eq. 7), and instantaneous panel and horizontal irradiances (Fig. 8B). An annual time series of energy production is computed and plotted by the function `solar_panel_annual.m` (Fig. 9).

The influence of clouds and atmospheric absorption, scattering and refraction is not taken into account, i.e. top-of-the-atmosphere (TOA) irradiance is used, and the center of the solar disk is considered. A 100 W nominal solar panel rating of 100 W is used in the greatly simplified energy production calculations (no temperature effects on panel performance are considered, and panel is assumed to produce more than 100 W when irradiance exceeds the standard of 1000 W). Clear view of the horizon in every direction is assumed. Students can be tasked to study the influence of and/or improve these assumptions. A major improvement that could be given as assignments of various kinds and complexity to more advanced students would be to combine the code presented here with knowledge of local climatology (e.g. clouds, water vapor profiles) and an atmospheric



radiative transfer model (e.g. SBDART - Ricchiazzi et al. (1998)) to improve the solar energy production estimates. Results
 235 can also be compared to the NREL solar resource maps (NREL (2020); Sengupta et al. (2018)). Furthermore, the effect of
 using simplified models of solar declination (rather than the full Meeus (1998) algorithms) (e.g. as given in Clack (2017) as
 a function of day of year) can be investigated. Finally, a natural development that can use the functions producing Fig. 8 is to
 task students with computing the times of local solar noon, sunrise and sunset, using various criteria such as the center of the
 solar disk at the mathematical horizon vs. at a given altitude below the horizon, to account for atmospheric refraction and the
 240 angular size of the solar disk.

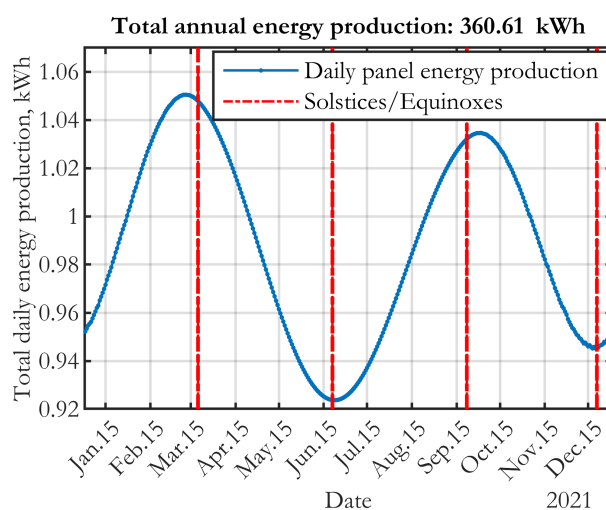


Figure 9. Time series of annual energy production using the defaults as described in the captions to Fig. 7 and Fig. 8 and in the function producing this plot: `solar_panel_annual.m`. Solstices and equinoxes are plotted as vertical dash-dot red lines.

2.6.1 Solar Panel Orientation Optimization

An important practical problem that needs to be solved in the installation of solar panels is deciding what panel orientation will maximize energy production, e.g. over year for a fixed panel. Using the solutions described in Sect. 2.6, the `solar_panel_orientation_optim.m` function optimizes the orientation of a fixed-mount solar panel to maximize
 245 annual energy production. Specifically, the function finds the optimal value of two variables: 1) the angle between the direction of the normal to the solar plane and the local vertical, i.e. the tilt of the solar panel, and 2) the azimuthal orientation of the solar panel in the horizontal plane, with respect to true North.

A hybrid optimization technique using genetic algorithms and an interior-point algorithm is used, illustrating the implementation of a generic constrained optimization technique that is useful for a wide variety of problems and in itself is
 250 pedagogically valuable. The user needs to have the Optimization© and Global Optimization© toolboxes in MATLAB© for this function to run. As an example, the optimization function returns a tilt of $\sim 31.35^\circ$ and azimuth of within less than 0.01° of 180° , using a default latitude of $\phi = 33^\circ 7' 45''$ N (and takes ~ 8 min to run in parallel (needs the Parallel Computing Tool-



box© of MATLAB©) on a 6-core 4 GHz Intel© processor, using a time step of 5 min). This indicates that to maximize energy production over an entire year, the panel should be facing southwards (as expected), and be tilted at approximately the same angle away from the vertical as the latitude, but $\sim 2^\circ$ less, somewhat favoring better exposure during the summer months.

Multiple exercises can be assigned to students using this optimization framework - the most straightforward one being to investigate optimal orientation for various latitudes. Students can also investigate the effect of the various assumptions used by improving upon them or changing them, for example by incorporating atmospheric effects (See Sect. 2.6) that are likely to change the optimization results. Students can also be tasked to come up with an analytical gradient-based solution to the optimization (which would be computationally much more efficient), perhaps using simplified models of solar coordinates (e.g. Clack (2017)). Further, students could be tasked to investigate the effects of changing the time step or taking or not taking into account Sun-Earth distance. More advanced students can investigate the effects of climatological atmospheric properties and the spectral response of a typical solar panel with respect to the spectral irradiance at the bottom of the atmosphere, as modeled by an atmospheric radiative transfer model (See Sect. 2.6) and perhaps using meteorological Reanalysis products to obtain data on atmospheric properties and climate at a given location. Students can also explore the effect of having several tilt options throughout the year (e.g. summer tilt vs. winter tilt - and when is it best to change the tilt), as well the effect of a tracking solar panel on energy production as compared to a fixed panel. All of these suggestions can be implemented using the existing code as starting framework. Conversely, students for whom delving into the code and computational methods is not appropriate can greatly benefit from the solar panel visualizations described in Sect. 2.6 and just running the code for various latitudes and panel orientations.

2.7 Solar Declination, Global Insolation and Daylength Plots

In this section, I present a few plots that are useful pedagogically in Earth science, physical geography, meteorology/climatology, astronomy, and related classes. A global visualization of mean daily top of the atmosphere (TOA) insolation as a function of date and latitude (Fig. 10)A is a frequently used plot that nicely illustrates seasonality on Earth and its variability with latitude, as well as the asymmetry of the hemispheres due to the eccentricity of Earth's orbit (the South Pole area receives higher insolation at the December solstice than the North Pole area at the June solstice) and the temporal phase shift of the seasons between the hemispheres. The figure presented here is enhanced in ways specifically targeting instructional value, e.g. students are taught to read a false color map of a variable that is a function of both a spatial and a temporal independent variables. Contours are also added to improve readability and can be used to teach isolines. Furthermore, the Equator and the solstices/equinoxes are drawn. This figure applies to contemporary Earth; instructors and students are referred to the Earth Orbit Model v2.1 (Kostadinov and Gilb (2014)) if interested in producing this plot for times in the geologic past or future, e.g. when teaching/studying the Milankovitch cycles and their effect on insolation and climate, glacial/inter-glacial cycles and related paleoclimatology topics.

The data used in Fig. 10A can be used to compute zonal annually averaged insolation and its temporal standard deviation, illustrating seasonality strength (Fig. 10B). Importantly, these data can be numerically integrated to obtain the globally and annually averaged TOA insolation, an essential variable controlling planetary energy balance and climate. This concept has

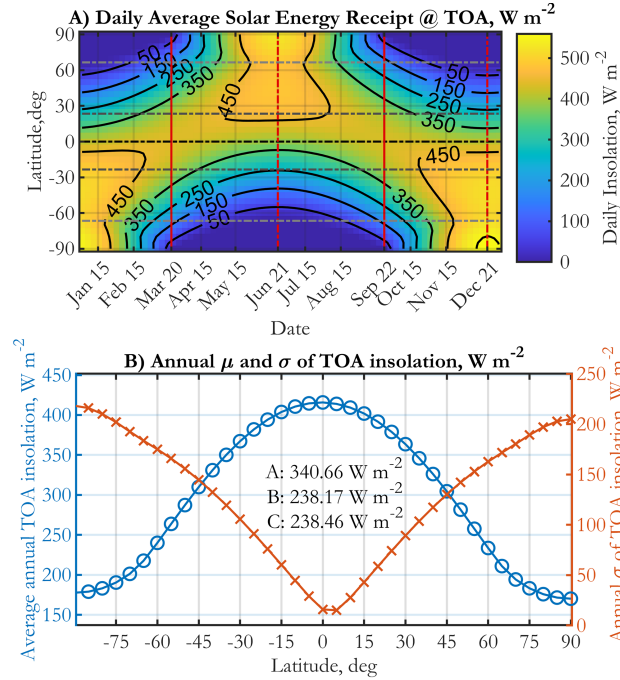


Figure 10. (A) Spatio-temporal distribution of daily average insolation on Earth, using insolation data from the Earth Orbit v2.1 model (Kostadinov and Gilb (2014)) for J2000. (B) Zonal annual means (left y-axis) and standard deviations (right y-axis) of insolation computed numerically from the data in panel A. The global annual average is shown as value A; the fraction of insolation absorbed by the Earth System (albedo assumed to be 0.3) is shown as value B (from the numerical integration) and compared to the direct analytical computation using the left-hand side of Eq. 8 (shown as value C). Figure panels are produced by the `plot_global_insolation.m` script. A value of TSI = 1361 W m⁻² is used.

gained importance for the general public and policy makers in the context of the anthropogenic climate change crisis. Earth's surface temperature can be estimated to first order based on the global planetary energy balance equation assuming black body radiation (e.g. Goosse (2015); Kasting (2010)):

$$290 \quad \frac{S_o}{4}(1 - A) = \sigma T^4 \quad (8)$$

where S_o is TSI (as in Eq. 7), A is Earth's albedo, T is Earth's temperature (in Kelvin), and σ is the Steffan-Boltzmann constant. This is arguably the most important equation of climate science and by extension all geosciences (Kasting (2010)). Note that this equation ignores the greenhouse effect and therefore significantly underestimates Earth's surface temperature, rather estimating Earth's "skin temperature" (Archer (2012)). The left-hand side of Eq. 8 is estimated numerically from the data in Fig. 10B by weighting the zonal averages by the cosine of the latitude, and is also computed directly. The small difference between these two values (Fig. 10B) is useful pedagogically to illustrate the inaccuracies introduced by numerical integration and the influence of choices of a spatio-temporal sampling grid.



Daylength (duration of daylight) as a function of latitude and date is illustrated in Fig. 11. The code uses the average solar declination for each date over four consecutive years to compute the average solar declination, δ , for each date, representative
 300 for a typical year. Daylength D in hours is then computed as:

$$D = \frac{2}{15} \cos^{-1}(-\tan \delta \tan \phi) \quad (9)$$

where ϕ is the latitude, and the inverse cosine result should be given in degrees. As previously discussed, Eq. 9 also considers the center of the solar disk being on the mathematical horizon as the sunrise/sunset times, and atmospheric refraction and twilight are not considered. It is derived by setting $h = 0^\circ$ in Eq. 4. Students should be encouraged to make more sophisticated
 305 sunrise/sunset estimates (see Sect. 2.6) or obtain sunrise/sunset times from, e.g., the NOAA Solar Calculator (NOAA (2020)) and compare the results. Fig. 11 also shows the solstices/equinoxes and solar declination, referred to in the plot as the subsolar point, making it suitable for use in introductory physical geography and Earth science classes for non-majors where introduction of additional astronomical terms such as declination may not be desirable.

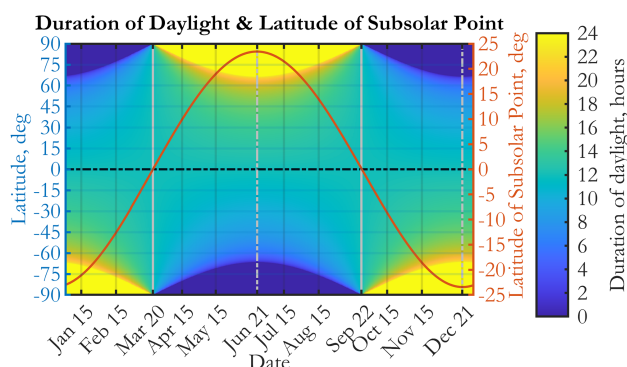


Figure 11. A plot of global daylength (duration of daylight, in hours) as a function of date and latitude. The solstices and equinoxes are indicated by vertical gray lines and solar declination is plotted as a function of date (right y-axis); it is referred to as latitude of the subsolar point in the plot. The plot is produced by the function `plot_declination_daylength.m`. The accompanying function `plot_declination.m` can be used to produce a standalone time series of just declination.

3 Concluding Remarks

310 In this manuscript, I introduce *AstroGeoVis v1.0* - software written MATLAB© that performs positional astronomy calculations of particular interest to the Earth sciences and renewable energy applications, i.e. focusing on Sun-Earth geometry, daily and annual paths of the Sun on the celestial sphere, seasons, and related concepts. The primary intended use of *AstroGeoVis v1.0* is pedagogical - multiple visualizations of instructional value are presented and the manuscript and code contain many ideas for applications in the classroom, including presenting a specific complete assignment in the case of the Solar Declination project
 315 (Sect. 2.1). Applications in the classroom are possible in a wide variety of fields and instructional contexts, and can range



from simply using the provided figures in class to illustrate often challenging concepts, to using the code to give students more advanced physical geography, Earth science, remote sensing/GIS, scientific computing, astronomy, mathematics, and related tasks. The author has used many of the visualizations here in the classroom and in assignments. Students generally respond favorably to them and indicate in course evaluations that visual aids and especially video materials are very helpful for their learning. However, care has to be taken not to introduce plots, terminology and material that is too technical for the particular classroom setting, e.g. a general education class with primarily non-STEM majors. A significant advantage of *AstroGeoVis v1.0* is that the code is open source and commented, and is itself of significant instructional value, giving instructors and students opportunities to dynamically generate/modify figures and inspect some of them in 3D with PTZ capability. Importantly, the computational methods can be inspected and instructors and/or students can perform quality control and introduce further developments.

Code availability. *AstroGeoVis v1.0* is made freely available (with a CC BY-NC-SA 4.0 license) in a GitHub© repository, archived at Zenodo© at the following URL: <https://doi.org/10.5281/zenodo.4393741>. Data needed to run *AstroGeoVis v1.0* is included with the code.

Video supplement. Example daily and annual animations of the terminator are included with the code.

Appendix A: Technical & License Information, & Description of Key Utility Scripts in *AstroGeoVis v1.0*

AstroGeoVis v1.0 is free to use, distribute and modify for non-commercial purposes under the Creative Commons BY-NC-SA 4.0 license. The author requests to be notified if any modified copies or derived works are to be distributed to third parties. Any such modifications must be clearly documented and stated properly.

To run the functions/scripts of *AstroGeoVis v1.0*, no installation is required. Simply download the folder containing all m-files, and make sure your MATLAB© working directory is pointing to that folder, or put it on your path. Run the function/script of interest on the command prompt using the appropriate arguments as described in the code comments (some can be omitted and defaults will be used).

The function `date2jd_vec_v2020.m` converts a date and time instant to Julian day (JD). The functions `sidereal_time.m` and `solar_coord.m` compute the sidereal time and solar right ascension, declination and the distance to the Sun for a given moment in JD. These functions use the Meeus (1998) algorithms. Note that figures produced by *AstroGeoVis v1.0* will have a slightly different appearance (fonts, axes labels/titles/legends presence and exact wording, etc.) than those in this manuscript for formatting reasons (to ensure figures fit in one column for compactness). No information or data of substance is different.



Appendix B: Useful Resources for Further Reading/Study

In addition to the sources cited in the manuscript and code, here I list a few resources that are useful for further reading, research,
345 and instruction. As *AstroGeoVis v1.0* development was independent of these resources, they could be used for verification and comparison.

- The timeanddate.com website (timeanddate.com (2020)), contains a plethora of astronomical information and visualiza-
tions and related tools and is an excellent teaching resource.
- US Naval Observatory Astronomical Applications (USNO (2020)).
- 350 – Explanatory Supplement to the Astronomical Almanac, (Urban and Seidelmann (2013)).
- Stellarium© planetarium software, (Stellarium (2020)).
- Two classical reference textbooks on spherical/positional astronomy are Smart (1977) and Green (1985).
- University of Oregon Solar Radiation Monitoring Laboratory SunChart ©, (SRML (2020)).

Author contributions. T.S.K. designed the study, wrote the code, and wrote the manuscript.

355 *Competing interests.* The author declares no competing interests.

Disclaimer. The *AstroGeoVis v1.0* software is supplied "as is". No warranty is given, express or implied, of fitness for any purpose. Under
no circumstances shall the author or his institution be liable to anyone for direct, indirect, incidental, consequential, special, exemplary, or
any other kind of damages (however caused and on any theory of liability, and including damages incurred by third parties), arising from or
relating to this software, or user's use, inability to use, or misuse of the software, or errors of the software. This software is not guaranteed
360 to be error-free and is not meant to be used in any mission-critical applications. Use at your own risk and verify with other sources when appropriate.

Acknowledgements. The author thanks California State University San Marcos (CSUSM) for providing support for this research. He thanks
the University of Richmond and the Andrew W. Mellon Foundation for providing support for development of earlier versions of some parts
of this work. He also thanks the students of University of Richmond Fall 2012 GEOG 250 class for collecting data used here as an example.
365 Further, he thanks his CSUSM students in the 2018-2020 period for providing feedback on the use of some of these visualizations in the
classroom and on the solar declination project.



The coastlines displayed on maps in *AstroGeoVis v1.0* use the high resolution L1 and L6 layers of the GSHHG v2.3.7 coastline data set Wessel and Smith (1996). The `generate_rot_m.m` script and the global insolation data in Sect. 2.7 are from the Earth Orbit v2.1 model of Kostadinov and Gilb (Kostadinov and Gilb (2014)), which uses the Laskar et al. (2004) Laskar, J. et al. (2004) orbital parameters to produce the insolation data.

The author also wishes to thank Jean Meeus for producing the very useful *Astronomical Algorithms* (Meeus (1998)), as well as Harish Vedantham and Martin Medina for the many useful discussions throughout the years that have contributed to the author's knowledge of the subject. The author thanks his astronomy teacher, Vanya Angelova, for being instrumental in developing his knowledge and interests in astronomy. He thanks Wikipedia© and its contributors for providing multiple relevant articles that are a great first step in research.

All coding, computations and visualizations were done in MATLAB©. This paper was typeset in L^AT_EX in Overleaf©. The author thanks Stackexchange© and its contributors for multiple L^AT_EX tips. Part of the electrical energy needed for *AstroGeoVis v1.0* development was produced by solar photovoltaics.



References

- Archer, D.: Global Warming, Understanding the Forecast, 2nd Edition, John Wiley and Sons, Inc., 2012.
- 380 Berger, A., Loutre, M.-F., and Yin, Q.: Total irradiation during any time interval of the year using elliptic integrals, *Quaternary Science Reviews*, 29, 1968 – 1982, <https://doi.org/https://doi.org/10.1016/j.quascirev.2010.05.007>, <http://www.sciencedirect.com/science/article/pii/S0277379110001435>, 2010.
- Christopherson, R. W.: *Geosystems: An Introduction to Physical Geography* (8th Edition), Pearson, 2011.
- Clack, C. T.: Modeling solar irradiance and solar PV power output to create a resource assessment using linear multiple multivariate regression, *Journal of Applied Meteorology and Climatology*, 56, 109–125, <https://doi.org/10.1175/JAMC-D-16-0175.1>, 2017.
- 385 Foster, G. L., Royer, D. L., and Lunt, D. J.: Future climate forcing potentially without precedent in the last 420 million years, *Nature Communications*, 8, 1–8, <https://doi.org/10.1038/ncomms14845>, 2017.
- Goosse, H.: *Climate System Dynamics and Modelling*, Cambridge University Press, 2015.
- Green, R. M.: *Spherical Astronomy*, Cambridge University Press, 1985.
- 390 Kasting, J.: *How to Find a Habitable Planet*, Princeton University Press, 2010.
- Kopp, G. and Lean, J.: A New, Lower Value of Total Solar Irradiance: Evidence and Climate Significance, *Geophysical Research Letters*, 38, <https://doi.org/10.1029/2010GL045777>, 2011.
- Kostadinov, T. S. and Gilb, R.: Earth Orbit v2.1: a 3-D visualization and analysis model of Earth's orbit, Milankovitch cycles and insolation, *Geoscientific Model Development*, 7, 1051–1068, <https://doi.org/10.5194/gmd-7-1051-2014>, [https://gmd.copernicus.org/articles/7/1051/](https://gmd.copernicus.org/articles/7/1051/2014/) 2014/, 2014.
- 395 Kostadinov, T. S., Milutinović, S., Marinov, I., and Cabré, A.: Carbon-based phytoplankton size classes retrieved via ocean color estimates of the particle size distribution, *Ocean Science*, 12, 561–575, <https://doi.org/10.5194/os-12-561-2016>, <https://os.copernicus.org/articles/12/561/2016/>, 2016.
- Laskar, J., Robutel, P., Joutel, F., Gastineau, M., Correia, A. C. M., and Levrard, B.: A long-term numerical solution for the insolation quantities of the Earth, *A&A*, 428, 261–285, <https://doi.org/10.1051/0004-6361:20041335>, <https://doi.org/10.1051/0004-6361:20041335>, 2004.
- Meeus, J.: *Astronomical Algorithms* Second Edition, Willmann-Bell, Inc., 1998.
- NOAA: ESRL Global Monitoring Laboratory - Global Radiation and Aerosols: NOAA Solar Calculator, <https://www.esrl.noaa.gov/gmd/grad/solcalc/>, (Accessed on 12/04/2020), 2020.
- 405 NREL: Solar Resource Data, Tools, and Maps | Geospatial Data Science | NREL, <https://www.nrel.gov/gis/solar.html>, (Accessed on 12/02/2020), 2020.
- Prša, A., Harmanec, P., Torres, G., Mamajek, E., Asplund, M., Capitaine, N., Christensen-Dalsgaard, J., Depagne, É., Haberreiter, M., Hekker, S., Hilton, J., Kopp, G., Kostov, V., Kurtz, D. W., Laskar, J., Mason, B. D., Milone, E. F., Montgomery, M., Richards, M., Schmutz, W., Schou, J., and Stewart, S. G.: NOMINAL VALUES FOR SELECTED SOLAR AND PLANETARY QUANTITIES: IAU 2015 RESOLUTION B3, *The Astronomical Journal*, 152, 41, <https://doi.org/10.3847/0004-6256/152/2/41>, <https://doi.org/10.3847/0004-6256/152/2/41>, 2016.
- 410 Ricchiazzi, P., Yang, S., Gautier, C., and Sowle, D.: SBDART: A Research and Teaching Software Tool for Plane-Parallel Radiative Transfer in the Earth's Atmosphere, *Bulletin of the American Meteorological Society*, 79, 2101–2114, [https://doi.org/10.1175/1520-0477\(1998\)079<2101:SARATS>2.0.CO;2](https://doi.org/10.1175/1520-0477(1998)079<2101:SARATS>2.0.CO;2), [https://doi.org/10.1175/1520-0477\(1998\)079<2101:SARATS>2.0.CO;2](https://doi.org/10.1175/1520-0477(1998)079<2101:SARATS>2.0.CO;2), 1998.



- 415 Sengupta, M., Xie, Y., Lopez, A., Habte, A., Maclaurin, G., and Shelby, J.: The National Solar Radiation Data Base (NSRDB), Renewable and Sustainable Energy Reviews, 89, 51 – 60, <https://doi.org/https://doi.org/10.1016/j.rser.2018.03.003>, <http://www.sciencedirect.com/science/article/pii/S136403211830087X>, 2018.
- Smart, W. M.: Textbook on Spherical Astronomy, 6th Edition, Cambridge University Press, 1977.
- SRML: Univ. of Oregon SRML: Sun chart program, <http://solardat.uoregon.edu/SunChartProgram.html>, (Accessed on 12/16/2020), 2020.
- 420 Stellarium: Stellarium Astronomy Software, <http://stellarium.org/>, (Accessed on 12/16/2020), 2020.
- timeanddate.com: timeanddate.com, <https://www.timeanddate.com/>, (Accessed on 12/16/2020), 2020.
- Urban, S. and Seidelmann, P.: Explanatory supplement to the Astronomical almanac, University Science Books, 2013.
- USNO: Astronomical Applications — Naval Oceanography Portal, <https://www.usno.navy.mil/USNO/astronomical-applications>, (Accessed on 12/16/2020), 2020.
- 425 Vincent, F.: Positional Astronomy: Conversion between horizontal and equatorial systems, <http://star-www.st-and.ac.uk/~fv/webnotes/chapter7.htm>, (Accessed on 11/16/2020), 2003.
- Wessel, P. and Smith, W. H. F.: A global, self-consistent, hierarchical, high-resolution shoreline database, Journal of Geophysical Research: Solid Earth, 101, 8741–8743, <https://doi.org/https://doi.org/10.1029/96JB00104>, <https://agupubs.onlinelibrary.wiley.com/doi/abs/10.1029/96JB00104>, 1996.